ISSN 0016-7029, Geochemistry International, 2007, Vol. 45, No. 11, pp. 1124–1130. © Pleiades Publishing, Ltd., 2007.
Original Russian Text ©L.P. Plyusnina, G.G. Likhoidov, Zh.A. Shcheka, 2007, published in Geokhimiya, 2007, No. 11, pp. 1216–1222.

Experimental Modeling of Platinum Behavior under Hydrothermal Conditions (300–500°C and 1 kbar)

L. P. Plyusnina, G. G. Likhoidov, and Zh. A. Shcheka

Far East Geological Institute, Far East Division, Russian Academy of Sciences, pr. Stoletiya Vladivostoka 159, Vladivostok, 690022 Russia

e-mail: lplyus@hotmail.com

Received May 4, 2006

Abstract—The behavior of Pt was studied in the Pt–Fe–S–Cl–H_2O, Pt–Fe(Ni)–As–S–Cl–H_2O, and Pt–Ni–As–Cl–H_2O systems. Kinetic experiments showed that the addition of As and S to the system changes the character of Pt complexing and results in a decrease in the bulk Pt content in the solutions. The intermediate complexes that formed during this process disproportionated to produce cooperite and sperrylite. Under the experimental *P-T*-μ_i conditions, the hydrothermal mobility of Pt was mainly provided by its hydrosulfide complexes with a definite participation of chloride complexes. The presence of Ni in the system lowers the redox potential and Pt solubility and prevents the formation of Pt phases, while Ni sulfides and arsenides crystallize copiously. The behavior of Pt and Au in hydrothermal systems and mechanisms of hydrothermal formation of noble metal minerals were considered.

DOI: 10.1134/S0016702907110055

INTRODUCTION

The concepts on the diversity of migration conditions of platinum group metals (PGE) in the magmatic, fluid–postmagmatic, and hydrothermal ore-forming systems have recently received considerable attention [1]. The discovery of hydrothermal Pt deposits raised the need to quantify its transport properties in complex solutions and geochemical barriers promoting its precipitation. Up to now, the solubility of Pt under hydrothermal conditions has been studied in $NaCl/H_2SO_4$ solutions under vapor-saturated conditions in relatively simple systems at T < 350°C [2–4]. This paper addresses the behavior of Pt, including its complexation, at 300–500°C and a pressure of 1 kbar in complex Cl–S–As-bearing aqueous systems.

To better approach natural conditions, oxygen fugacity and activities of sulfur and arsenic were buffered by mineral assemblages. The model interaction of ore-bearing chloride solutions with sulfide and sulfoarsenide assemblages allowed us to estimate the role of Cl, S, and As in Pt transport.

EXPERIMENTAL

The experiments were conducted using the ampoule–autoclave technique. The walls of sealed Pt ampoules (10 × 80 × 0.2 mm) served as a Pt source. A buffer mixture (~200 mg) was loaded directly into the solution, because the double capsule technique is inefficient below 500°C [5]. The experiments lasted from 10–15 days at 500–400°C to 30 days at 300°C. The duration of kinetic experiments was 24–720 hours. After solution quenching, Pt_{aq} was extracted into alkylaniline and analyzed by atomic absorption and atomic emission spectroscopy at the analytical center of the Far East Geological Institute, Far East Division of the Russian Academy of Sciences. Depending on the method, the analytical sensitivity varied within 0.1–0.2 μg, and the total relative error was no higher than 10%. The experimental solid phases were investigated by X-ray diffraction on a DRON-3 instrument, and the chemical composition of synthesized phases was analyzed on a Pt substrate using a CamScan MV 2300 (VEGA TS 5130 MN) microprobe at the Institute of Experimental Mineralogy, Russian Academy of Sciences (Chernogolovka).

EXPERIMENTAL RESULTS

Pt–Fe–Cl–S–O–H System

The fugacities of sulfur and oxygen in experiments with metallic Pt were buffered by the pyrite–pyrrhotite–magnetite (PPM) assemblage. Their *in situ* values were calculated from the final composition of pyrrhotite using the method [6] based on the interplanar spacing $d_{(102)}$ of quenched pyrrhottie (Table 1). It is known that the PPM assemblage monitors the pH of solutions at weakly acid–near-neutral values [7]. The starting liquids consisted of water and 1 *m*NaCl and 0.1 *m*HCl solutions. After the completion of the experiment, black coating was observed on the walls and small clippings of Pt ampoules (substrate) which were used for the X-ray analysis of newly formed minerals. We found cooperite (*Coop*) containing 85.2 ± 0.5 wt % Pt, 14.7 ± 0.3 wt % S, and up to 0.2 wt % Fe and corresponding to

the formula $Pt_{0.95}Fe_{0.01}S_{1.05}$. The rate of its crystallization increases with increasing temperature. In particular, a discontinuous 3-nm-thick layer of cooperite was formed at 300°C within three week, whereas a continuous film up to 10–15 nm thick was observed in the products of 10–12-day experiments at 500°C. In this connection, a series of kinetic experiments was carried out on the dissolution of metallic Pt in water at 300°C, when the rate of *Coop* crystallization was minimal. The solubility of *Coop* was measured in ampoules, which were preliminarily lined with PtS at 500°C. As a result, the kinetic dissolution curves of metallic Pt and PtS were constructed (Fig. 1). The bulk Pt concentration in the solution is controlled by the dissolution of metallic Pt between the starting point and the maximum, dissolution of Pt_{met} and PtS after the appearance of *Coop*, and cooperite solubility after the complete coating. The maximum on the kinetic curve at this stage is related to the formation of the hydroxide complex $Pt(OH)_2^0$ [8]. As the medium becomes saturated with respect to the components of the PPM assemblage, the activity of hydrosulfides increases and the bulk Pt concentration decreases, thus defining the shape of the maximum on the curve. In the chloride medium, Pt dissolution is also controlled by the formation of chloride Pt complexes (Table 2). Variations in bulk Pt concentrations under the experimental condition are shown by the surface in the $\log m$Pt–composition–temperature diagram (Fig. 2).

Complex compounds containing several ligands in the coordination sphere can be produced by the interaction between hydroxide, chloride, and hydrosulfide Pt complexes [9]. Such mixed complexes are unstable and disproportionate with time to precipitate PtS according to the reaction

$$\begin{aligned} &Pt(OH)_2 + xH_2S^0 + yHS^- \\ &\longrightarrow (PtS \times xH_2(S\times yHS^-))^{y-} + H_2O + 0.5O_2 \\ &\longrightarrow xH_2S + yHS^- + PtS\downarrow. \end{aligned}$$

The stoichiometry of the proposed multinuclear Pt complexes is, of course, hypothetical. Such a mechanism of *Coop* crystallization is indirectly supported by the precipitation of CuS from copper hydrosulfide solutions at 200°C [10]. This explains the type of kinetic curves (Fig. 1) and the stepwise crystallization of *Coop* from a solution.

The solubility of *Coop* illustrates the weak dependence of bulk Pt concentration in solutions on their initial acidity (Table 2). In addition, the Pt content in "pure" water slightly increases with temperature, whereas the opposite behavior is observed in chloride solutions.

Table 1. Sulfur and oxygen fugacities calculated from pyrrhotite composition

T, °C	$d_{(102)}$, Å	m_{FeS}	a_{FeS}	$\log f_{S_2}$	$\log f_{O_2}$
300	2.065	0.940	0.53	–10.73	–32.16
400	2.060	0.035	0.50	–7.00	–26.01
500	2.056	0.930	0.48	–4.17	–20.63

Note: d is the interplanar spacing, and m and a are the mole fraction and activity of troilite in pyrrhotite, respectively.

Pt–Fe–Cl–S–As–O–H System

To estimate the effect of As on the behavior of Pt in hydrothermal conditions, bulk Pt concentration was studied in chloride–sulfide–arsenic solutions, using 0.1 *m*HCl as a starting solution and the arsenopyrite (*Apy*)–pyrrhotite–magnetite (APyPM) buffer assemblage. About 5 mg of As_{met} was added to saturate the system in As. The starting *APy* had the following composition (wt %): As 42.05, Fe 35.90, S 20.97, and Ni 0.59. It was assumed that the APyPM assemblage maintained sulfur and oxygen fugacity at the same level as was calculated for the PPM buffer. This is justified by the phase diagram of the As–S–O–H system in the $\log f_{O_2}$–T coordinates [11].

Light gray films of sperrylite (*Sper*-$PtAs_2$) were observed on the substrate and inner walls of platinum ampoules in the products of 300, 400, and 500°C experiments. Sperrylite was identified using an X-ray Gandolfi camera and confirmed by microprobe analysis. Euhedral prismatic *APy* with a Pt admixture was formed together with *Sper* at 400°C. The microprobe investigation showed the predominance of prismatic cooperite crystals with an admixture of Fe and As in the run products at the 500°C isotherm. The analysis of films on the substrate showed that euhedral thin-prismatic crystals of newly formed pyrrhotite contain an admixture of Pt and As (Table 3). Pyrite was formed at the expense of arsenopyrite, as indicated by a sharp

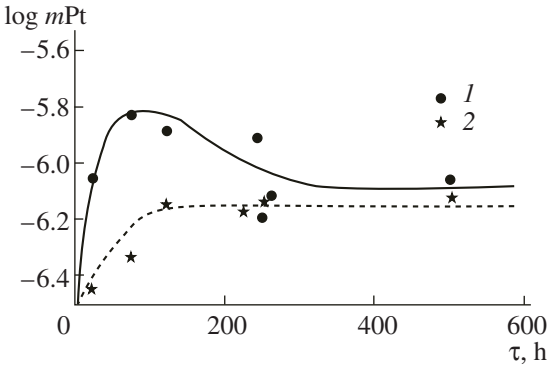

Fig. 1. Kinetic curves for the dissolution of (*1*) Pt and (*2*) Pt monosulfide and changes in the bulk content of Pt in the system.

Table 2. Bulk Pt concentration ($\log mPt$) in quenched solutions (P_{tot} = 1 kbar)

Solution	300°C	400°C	500°C
		Pt_{met}	
H_2O	–5.90 ± 0.30(6)	–5.85 ± 0.17(2)	–5.57 ± 0.20(2)
1*m*NaCl	–5.48 ± 0.27(2)	–5.07 ± 0.40(3)	–6.02 ± 0.30(2)
0.1*m*HCl	–5.30 ± 0.40(2)	–4.94 ± 0.30(2)	–5.69 ± 0.30(2)
		PtS	
H_2O	–6.16 ± 0.25(6)	–5.87 ± 0.16(2)	–5.72 ± 0.30(4)
1*m*NaCl	–5.81 ± 0.30(2)	–6.12 ± 0.40(3)	–6.54 ± 0.15(3)
0.1*m*HCl	–5.34 ± 0.15(3)	–5.47 ± 0.30(3)	–5.59 ± 0.15(3)

Note: *m* is the molality (number of moles per 1 kg H_2O), and the numbers in parentheses are the numbers of determinations.

decrease in the content of arsenopyrite in the run products.

Judging from the thickness of the newly formed layers, the rate of spontaneous crystallization significantly increased with increasing temperature. In particular, sperrylite analyses from the products of the 300 and 400°C experiments lasting less than three and two weeks, respectively, showed more than 1 a.f.u. Pt, which is related to the contribution of the Pt substrate. Stoichiometric sperrylite ($Pt_{0.90}Fe_{0.10}As_{1.60}S_{0.40}$) with high sulfur content was obtained in 10-day experiments at 500°C.

Similar to *Coop*, the maximum of Pt_{aq} in 0.1 *m*HCl solution buffered by the APyPM assemblage was observed at the beginning of the kinetic curve, before the crystallization of Pt arsenide and sulfide (Fig. 3). Similar to the case with cooperite, the shape of the dissolution curve can be explained in terms of the theory of an intermediate activated complex [12]. In a more complex system, hydroxide and chloride Pt complexes interact with sulfoarsenide ones. The rate of dissolution of the APyPM assemblage appeared to be lower than that of metallic Pt. The stoichiometry of mixed complexes in the chloride–sulfide–arsenide solutions may be fairly complicated; this problem requires special study and is not discussed in this paper. The bulk Pt and As contents measured in the quenched solutions is given in Table 4. Owing to analytical difficulties, satisfactory results for bulk As_{aq} content were obtained only at 400°C.

Pt–Fe–Ni–Cl–S–As–O–H System

The effect of accompanying metals on Pt transfer in chloride–sulfide–arsenide solutions was estimated by adding Ni to the system. It is known that Ni sulfides and arsenides often accompany PGE mineralization [13]. In this case, a mixture of Ni–NiO–APy–As_{met} was used as a starting mineral assemblage. X-ray phase analysis revealed newly formed magnetite, Ni sulfides (heazlewoodite, Ni_3S_2), and Ni arsenides (nickelarsenide, Ni_5As_2). Pt compounds were never found in the solid experimental products. A continuous film of metallic Ni with a Pt content below the detection limit was formed on the ampoule walls and Pt substrate. Variations in bulk Pt concentrations under these conditions are shown in Table 4.

The compositional changes of solid charges during the experiments suggested the following buffer reaction: $6FeAsS + 6NiO + 12Ni + O_2 = 2Fe_3O_4 + Ni_3S_2 + 3Ni_5As_2$. This reaction controls the activity of S and As, while the oxygen fugacity is maintained at a lower level

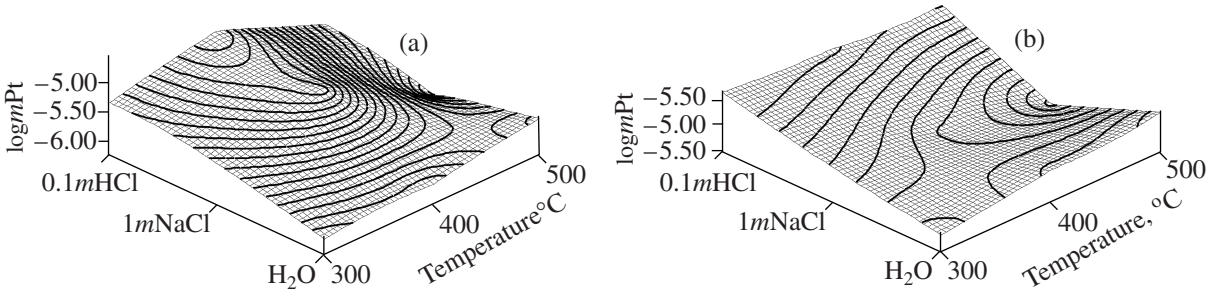

Fig. 2. Surfaces of variations in the bulk concentration of Pt in the water–chloride medium buffered by PPM during the dissolution of (a) Pt_{met} and (b) PtS at P_{tot} = 1 kbar.

compared with the experiments with APyPM mixture. The latter is confirmed by the simultaneous decrease in Pt_{aq} content and increase in As_{aq} reported by Pokrovskii et al. [14]. The absence of newly formed cooperite and sperrylite among the run products is probably caused by the extremely low solubility of Pt under these conditions and higher Ni affinity to S and As.

Pt–Ni–Cl–As–O–H System

To estimate more correctly the effect of As on Pt behavior, sulfur was excluded from the system, and 0.1 *m*HCl solution interacted with the Ni–NiO–As_{met} starting mixture. The experimental products contained the Ni–NiO–Ni_5As_2 assemblage. Metallic Ni also precipitated on the ampoule walls in the absence of Pt-bearing phases. The following reaction can be proposed on the basis of experimental products: $4Ni + NiO + 2As \rightleftharpoons Ni_5As_2 + 0.5O_2$ [15]. The $\log f_{O_2}$ value in a 0.1 *m*HCl solution in the presence of metallic As at 300°C is calculated as –47.9 [16]. The solubility of Pt in this medium is at the detection limit of the AA-6200 spectrophotometer (Table 4), which attests to the insignificant influence of chloride and arsenide complexes on Pt mass transfer under reducing conditions.

DISCUSSION AND CONCLUSIONS

The following conclusions can be drawn from the position of the maximum Pt content as a function of solution composition and temperature (Fig. 2a, Table 2). Based on the solubility surface, an increase in the maximum Pt content in the chloride solution as compared to the "pure" water indicates that chloride Pt complexes were formed since the beginning of Pt dissolution and that the acid environment was most favorable. The isopleths of the dissolution surface indicate that the appearance of hydrosulfides and an increase in their activity shift the extreme maximum toward lower temperatures. This is accompanied by a decrease in bulk Pt concentration in the solutions mainly at the expense of a decrease in the activity of chloride species. A similar situation is typical of the subcritical field, where the low chloride solubility of Pt (<1 ppb) was related to the formation of "aqueous sulfides" [2]. In our case, a decrease in Pt solubility was related to the dissolution of Py and Po of the PPM assemblage. The bulk Pt concentration reaches a maximum and then decreases to the values controlled by PtS solubility. The evolution of cooperite solubility is illustrated by its solubility surface in the coordinates of experimental parameters (Fig. 2b, Table 2).

The results of experiments at 200–350°C in the $H_2S^0/HS^-/SO_4^{2-}$ bearing solutions also demonstrated a decrease in the bisulfide solubility of Pt with increasing temperature, which was related to a possible increase in the role of chloride complexes [4]. A different situation was observed in the P-T-μ_i range studied. The bisulfide solubility of Pt in a chloride-free medium increases distinctly with increasing temperature (Fig. 2b, Table 2). The appearance of chlorides in the system at lower temperature (300°C) confirms the suggestion of these authors for the isobar studied by us. At the same time, the bulk Pt solubility at other isotherms shows both positive and negative changes and regularly increases only in an acid environment, in spite of an order of magnitude lower content of chlorides.

Table 3. Composition of newly formed phases at P_{tot} = 1 kbar (wt %)

Mineral (t, °C)	Pt	Fe	S	As	Σ
Sper (400)	60.40	2.61	2.14	34.12	99.27
APy (400)	4.96	34.30	18.10	42.34	99.70
Sper (500)	54.78	5.21	5.01	33.82	98.82
Coop (500)	79.50	3.26	16.00	1.65	100.41
Po (500)	2.20	57.82	37.59	2.36	99.97

At the kinetic stage of dissolution in a complex medium, the bulk Pt concentration decreases with the appearance of hydrosulfides mainly at the expense of chloride species. Thus, the participation of chlorides in this process is beyond doubt. Their contribution is positive in an acid medium and is characterized by an alternating sign in the near-neutral (1 *m*NaCl) region. A significant increase in the chloride solubility of Pt with increasing temperature (200 ⟶ 500°C) was noted only in a sulfur-free medium at $\log f_{O_2} > -20$ [17].

The bulk Pt content is further decreased by the addition of As to the sulfide–chloride system. A chloride medium in equilibrium with arsenopyrite is more reducing as compared with the pyrite-bearing system, at least at 300–400°C [14]. This explains the observed decrease in the bulk Pt concentration in the quenched solutions. This process is accompanied by the crystallization of sperrylite with arsenopyrite and, at a higher

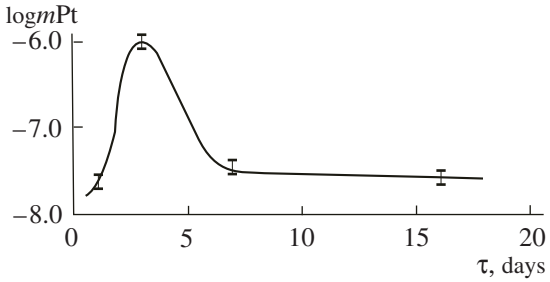

Fig. 3. Kinetic curve showing variations in the bulk concentration of Pt in 0.1 *m*HCl solution in the presence of the APyPM assemblage at 500°C and 1 kbar. The vertical bars show uncertainty intervals.

Table 4. Pt concentration in 0.1 *m*HCl solution as a function of temperature and the compositional evolution of the solid charge during experiments

$\log mPt^{aq}$			$\log mAs^{aq}$	Starting assemblage	Newly formed phases
300°C	400°C	500°C	400C		
–6.28 ± 0.15	–6.40 ± 0.20	–7.60 ± 0.10	–5.60	APyPM	$PtAs_2$, PtS
–6.78 ± 0.30	–6.80 ± 0.30	n.d.	–4.82	NNO + APy + As	Fe_3O_4, Ni_3S_2, Ni_5As_2
–7.08 ± 0.30	–7.49 ± 0.30	n.d.	n.d.	NNO + As	Ni_5As_2

temperature, cooperite with pyrrhotite (Tables 3, 4). Only scanty data are available on As speciation in sulfide and chloride solutions. It is suggested that arsenopyrite dissolves incongruently in H_2S-bearing aqueous solutions to form orthoarsenous acid according to the reaction $4FeAsS + 4H_2S^0 + 5O_2 + 2H_2O = 4FeS_2 + 4H_3AsO_3^0$ [11]. In addition, the speciation of As depends on the pH, $H_2S°$ activity, and redox potential of the system. An increase of a sulfur admixture in *Sper* with increasing temperature and the new formation of arsenopyrite indicate an increase in hydrosulfide activity and possible appearance of binuclear sulfide–arsenide complexes. There is an opinion that $H_2As_2S_4^0$ is the main species in neutral solutions, while $HAs_2S_4^-$ and $As_2S_4^{2-}$ are predominant in acid and weakly acid solutions [18]. The order of new mineral formation in the Pt–Fe–Cl–S–As–O–H system, *Sper* (300°C) ⟶ *Sper* + *APy* (400°C) ⟶ *Coop* + *Sper* + *Po* (500°C), and the evolution of mineral compositions (Table 3) indicate that the role of S increases with increasing temperature at the expense of As. It should be noted that cooperite is formed already at ~300°C in the As-free system [8].

The obtained results suggest that the hydrothermal mobility of Pt and the formation of its own minerals are controlled not only by the composition and evolution of ligand-forming components but also by the presence of other metals. This can be exemplified by nickel. As was noted above, cooperite and sperrylite are not formed in a Ni-bearing hydrothermal environment. The solubility of Pt decreases sharply under such conditions, and Ni sulfides and arsenides are actively formed. The incorporation of Pt in Ni sulfides and arsenides was suggested by many researchers [19]. For example, these minerals are main Pt hosts at the Pechenga deposits [20]. We failed to analyze the compositions of newly formed Ni sulfides and arsenides in view of their small sizes. It should be noted that cooperite in association with Ni sulfides typically occur in magmatic ores [13, 21]. At a temperature of about 300°C and lower, sperrylite associates with hydrothermal Cu sulfides (covellite, digenite, and bornite) at the Salt Chuck deposit, Alaska [22]. Similar to the experimentally studied As-bearing system, cooperite does not occur in this deposit, and the associated sulfides have extremely low Ni contents.

Although the number of Pt deposits of undoubtedly hydrothermal genesis has increased in the past years [23], it is significantly smaller than the number of hydrothermal gold deposits. It is thought that this could be related to the fact that the solubility of Au under hydrothermal conditions is two orders of magnitude higher than that of Pt [4]. Some researchers argued that gold is transported mainly with hydrosulfide complexes [24, 25]. There is an opinion that an increase in As content leads to an increase in Au solubility; therefore, under reducing conditions, As together with S plays a leading role in Au transport [18]. In chloride–sulfide solutions buffered by the PPM assemblage, the bulk concentration of Au increases with increasing temperature and chloride activity [26, 27]. In addition, composite chloride–bisulfide Au complexes are stable at temperatures of higher than 400°C (in contrast to the same Pt complexes) and could also contribute to this process [28, 29].

High-temperature (1100–1350°C) experiments on the partitioning of gold and platinum between fluid and basaltic melt demonstrated that the solubility of Pt in chloride fluids is higher than that of Au, and the extracting ability of chloride fluids with respect to noble metals increases with decreasing temperature [30]. Thus, chlorine plays the leading role in the mobilization and transportation of Pt at high temperature. However, the presence of sulfides and arsenides in natural hydrothermal environments affects this process. In particular, it was shown above that the activity of chloride Pt complexes is suppressed under reducing conditions imposed by the corresponding mineral assemblages. Since sulfide solubility of Pt is less than that of Au, Pt is less mobile under hydrothermal conditions. This underlies the differences in the geochemical behavior of these noble metals.

As was shown above, the change in Pt complexation with the appearance of S and As in the system leads to the crystallization of cooperite and sperrylite even from solutions with low Pt contents. The activities of S and As are controlled in such a case by the dissolution of sulfides and arsenides. Similar mechanisms, though related to changes in redox potential, operate during the crystallization of metallic Pt, which was established in a sulfide-free system [29]. The precipitation of noble metals under hydrothermal conditions was described for the first time for Au by Gammons [31]. This author

related the crystallization of metallic gold with a change from the complexes of monovalent Au to trivalent Au with decreasing temperature [32]. We believe that this scheme of changes in the character of complexing is applicable to Pt and may be universal. In particular, the appearance of S and As in the system leads to the crystallization of Pt sulfides and arsenides; a change in redox potential in chloride solutions causes the precipitation of metallic Pt [29]; and a change from monovalent to trivalent complexes of Au leads to the crystallization of Au_{met} [31]. This fact explains, in particular, the reasons for the hydrothermal formation of minerals that were previously considered as magmatic. In the general case, our results define geochemical barriers and the conditions of their realization in the corresponding natural settings.

ACKNOWLEDGMENTS

This study was supported by the Far East Division of the Russian Academy of Sciences (project no. 06-II-SO-08-029, "Geological and Genetic Models of Large-Scale Deposits of Noble, Base, and Trace Metals of the Northern Far East of Russia").

REFERENCES

1. D. A. Dodin, N. M. Chernyshov, and B. A. Yatskevich, *Deposits of Platinum-Group Metals in Russia (Nauka, St. Petersburg, 2000)* [in Russian].
2. C. H. Gammons, C. S. Bloom, and Y. Yu, "Experimental Investigation of the Hydrothermal Geochemistry of Platinum and Palladium. 1. Solubility of Platinum and Palladium Sulfide Minerals in $NaCl/H_2SO_4$ Solutions at 300°C," Geochim. Cosmochim. Acta **56**, 3881–3894 (1992).
3. C. H. Gammons, "Experimental Investigation of the Hydrothermal Geochemistry of Platinum and Palladium. IV. The Stoichiometry of Pt(IV) and Pd(II) Chloride Complexes at 100 to 300°C," Geochim. Cosmochim. Acta **59**, 1665–1668 (1995).
4. P. Pan and S. A. Wood, "Solubility of Pt and Pd Sulfides and Au Metal in Aqueous Bisulfide Solutions. II. Results at 200 to 350°C and Saturated Vapour Pressure," Mineral. Deposita **29**, 373–390 (1994).
5. I. M. Chou, "Oxygen Buffer and Hydrogen Sensor Techniques at Elevated Pressures and Temperatures," in *Hydrothermal Experimental Techniques*, Ed. by H. P. Eugster, (Wiley, New York, 1987), pp. 61–90.
6. N. I. Bezmen, L. B. Granovskii, and L. V. Sipavina, "Pyrrhotite–Magnetite Equilibrium as an Indicator of Equilibrium in Experiment," in *Essays on Physicochemical Petrology* (Nauka, Moscow, 1997), Vol. 6, pp. 34–45 [in Russian].
7. D. A. Crerar, N. J. Susak, M. Boresik, and S. Schwartz, "Solubility of the Buffer Assemblage Pyrite–Pyrrhotite–Magnetite in NaCl Solutions from 200 to 350°C," Geochim. Cosmochim. Acta **42**, 1427–1437 (1978).
8. L. P. Plyusnina, G. G. Likhoidov, and I. Ya. Nekrasov, "Platinum Behavior in the Aqueous Sulfide–Chloride Medium at 300–500°C and 1 kbar," Dokl. Akad. Nauk **370**, 99–101 (2000) [Dokl. Earth Sci. **370**, 86-88 (2000)].
9. V. I. Belevantsev, G. R. Kolonin, N. G. Vasil'eva, et al., "Possible Modes of Occurrence and Solubility of Gold in Ore-Forming Solutions," Tr. Inst. Geol. Geofiz. Sib. Otd. Akad. Nauk SSSR, No. 505, 83–118 (1982).
10. S. B. Romberger and H. L. Barnes, "Ore Solution Chemistry. III. Solubility of CuS in Sulfide Solutions," Econ. Geol. **65**, 901–919 (1970).
11. C. A. Heinrich and P. Eadington, "Thermodynamic Predictions of the Hydrothermal Chemistry of Arsenic, and Their Significance for the Paragenetic Sequence of Some Cassiterite–Arsenopyrite–Base Metal Sulfide Deposits," Econ. Geol. **81**, 511–529 (1986).
12. A. G. Stromberg and D. P. Semchenko, *Physical Chemistry* (Vysshaya shkola, Moscow, 1988) [in Russian].
13. S. M. Verryn and R. K. Merkle, "Cooperite, Braggite and Vysotskovite in the System PtS–PdS–NiS at 1100, 1000 and 900°C," Mineral. Petrol. **68**, 63–73 (2000).
14. G. S. Pokrovskii, S. Kara, and J. Roux, "Stability and Solubility of Arsenopyrite, FeAsS, in Crustal Fluids," Geochim. Cosmochim. Acta **66**, 2361–2378 (2002).
15. L. P. Plyusnina, G. G. Likhoidov, and A. I. Khanchuk, "Experimental Modeling of Platinum Behavior in the Pt–Fe–As–Cl–H_2O and Pt–Ni–As–Cl–H_2O Systems at 300–500°C and 1 kbar," Dokl. Akad. Nauk **405**, 105–107 (2005) [Dokl. Earth Sci. **405**, 1235-1237 (2005)].
16. V. I. Tikhomirova, A. V. Chichagov, and G. M. Akhmedzhanova, "Experimental Modeling of the Assemblage of Noble Metals with Intermetallides Containing Group V Elements," in *Experimental Mineralogy," (Nauka, Moscow, 2004), Vol. 1, pp. 364–375* [in Russian].
17. L. P. Plyusnina, "The Effect of Phase Transformations in the System Mn–O_2–H_2O on the Solubility of Platinum and Gold at 200–400°C and 1 kbar," Geokhimiya, No 1, 80–86 (2002) [Geochem. Int. **40**, 72–78].
18. I. Ya. Nekrasov, *Geochemistry, Mineralogy, and Genesis of Gold Deposits* (Nauka, Moscow, 1991) [in Russian].
19. N. M. Chernyshov, *Platinum-Bearing Associations of the Kursk–Voronezh Region* (Voronezh Univ., Voronezh, 2004) [in Russian].
20. V. V. Distler, A. A. Filimonova, T. L. Grokhovskaya, and I. P. Laputina, "Platinum Group Metals in the Copper–Nickel Ores of the Pechenga Ore Field," Geol. Rudn. Mestorozhd. **31**, 3–17 (1988).
21. A. B. Mostres, P. K. Hofmeyer, and G. A. Potgieter, "The PGM of the Merensky Reef at the Impala Platinum Mines," Econ. Geol. **77**, 1385–1394 (1982).
22. D. H. Watkinson and D. P. Melling, "Hydrothermal Origin of the Platinum Mineralization, Alaska," Econ. Geol. **87**, 175–184 (1992).
23. V. V. Distler, M. A. Yudovskaya, V. A. Prokof'ev, and Ya. V. Mun, "Hydrothermal Platinum Mineralization of the Waterberg Deposit (Transvaal, South Africa)," Geol. Rudn. Mestorozhd. **42**, 363–376 (2000) [Geol. Ore Dep. **42**, 328–339].
24. T. M. Seward, "The Hydrothermal Geochemistry of Gold," in *Gold Metallogeny and Exploration*, Ed. by R. P. Foster (Blackie, Glasgow, 1991), pp. 37–62.
25. L. G. Benning and T. M. Seward, "Hydrosulfide Complexes of Au(I) in Hydrothermal Solutions from 150–400°C and

500–1500 Bars," Geochim. Cosmochim. Acta **60**, 1849–1871 (1996).

26. F. Gibert, M. L. Pascal, and M. Pichavant, "Gold Solubility and Speciation in Hydrothermal Solutions: Experimental Study of the Stability of Hydrosulfide Complexes of Gold at 350°C to 450°C and 500 Bars," Geochim. Cosmochim. Acta **62**, 2931–2948 (1998).

27. G. G. Likhoidov and I. Ya. Nekrasov, "Gold Solubility in Complex Sulfide–Chloride Fluids at 300–500°C and P_{total} = 1 kbar," Geokhimiya, No. 4, 394–403 (2001) [Geochem. Int. **39**, 347–355 (2001)].

28. R. R. Loucks and J. A. Mavrogenes, "Gold Solubility in Supercritical Hydrothermal Brines Measured in Synthetic Fluid Inclusions," Science **284**, 2159–2163 (1999).

29. G. G. Likhoidov, L. P. Plyusnina, J. A. Scheka, and T. B. Aphanas'eva, "Experimental Study of Gold and Platinum Solubility in a Complex Fluid under Hydrothermal Conditions," Resour. Geol. **50** (2), 83–92 (2000).

30. N. S. Gorbachev, A. Naldrett, G. Brügmann, et al., "Experimental Study of PGE and Gold Partitioning between Solution and Melt at T = 1100–1350°C and P = 5 kbar," Dokl. Akad. Nauk **335**, 356–358 (1994).

31. Ch. H. Gammons, "Hydrothermal Synthesis of Gold Grains with Apparent Five-Fold Symmetry," Can. Mineral. **34**, 1–8 (1996).

32. Ch. H. Gammons and A. E. Williams-Jones, "The Solubility of Au–Ag Alloy + AgCl in HCl/NaCl Solutions at 300°C: New Data on Stability of Gold(1) Chloride Complexes in Hydrothermal Fluids," Geochim. Cosmochim. Acta **59**, 3453–3468 (1995).